

Ultralow-Concentration Electrolyte for Na-Ion Batteries

Yuqi Li,[†] Yang Yang,[†] Yaxiang Lu,^{*} Quan Zhou, Xingguo Qi, Qingshi Meng, Xiaohui Rong, Liquan Chen, and Yong-Sheng Hu^{*}



Cite This: *ACS Energy Lett.* 2020, 5, 1156–1158



Read Online

ACCESS |



Metrics & More

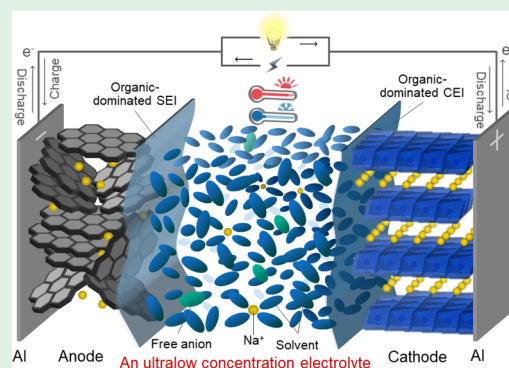


Article Recommendations



Supporting Information

ABSTRACT: Owing to the smaller Stokes radius and desolvation energy of Na^+ compared to those of Li^+ , an unusual ultralow-concentration electrolyte is proposed for Na-ion batteries to further reduce the cost and expand the working temperature range, benefiting from the low viscosity of a dilute electrolyte and the formed organic-dominated solid electrolyte interphase. The novel dilute electrolyte chemistry provides new solutions for the operation of rechargeable batteries under extreme conditions, which can accelerate the exploitation of low-cost and durable energy storage systems.



Electrolytes are indispensable in energy storage devices, and regulating electrolyte concentration is a key strategy for achieving functional design. In the past few years, increasing the salt concentration has been proven to be an effective solution for Li-metal batteries, aqueous batteries, *etc.* because of the special bulk and interface properties in salt-concentrated electrolytes (Figure 1a).^{1–4} On the opposite end, decreasing the salt concentration to form a super dilute electrolyte has not been explored yet, considering the possible concentration polarization⁵ from low ionic conductivity. Thus, the standard concentration of 1 M (mol/L) is still commonly used today.⁴ However, because of the smaller Stokes radius and desolvation energy of Na^+ than those of Li^+ , it is possible for Na-ion batteries (NIBs) to employ the low-concentration electrolyte to obtain enough kinetics performance.^{6,7} Furthermore, reducing the expensive salt content can effectively control the cost of NIBs (Figure S1),⁸ which is beneficial for application in grid storage. Herein, we propose using an ultralow-concentration electrolyte (0.3 M) for the practical Na-ion full cells for the first time, surprisingly, which achieves good performance in the wide working temperature range benefitting from the dilute electrolyte chemistry. This attractive electrolyte formulation was provided from an inverse design, offering new insights for solving the failure problem of rechargeable batteries under extreme conditions.

A series of electrolytes with different concentrations was prepared by dissolving NaPF_6 in ethyl carbonate (EC)/propylene carbonate (PC) (1:1 vol %) without extra additives

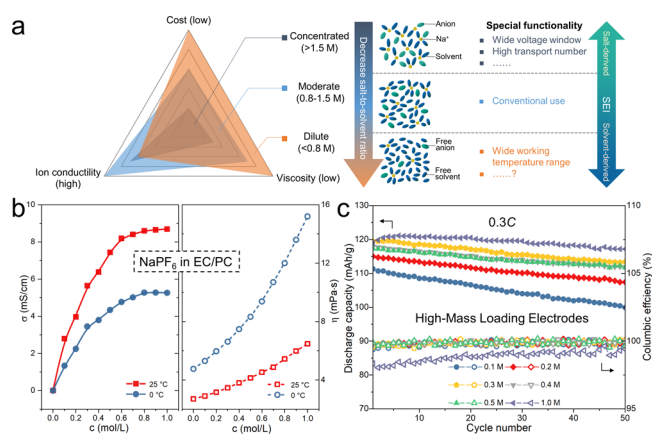


Figure 1. (a) Overview of the electrolytes from high concentration to lower concentration and the related variations about physicochemical properties, interactions between molecules/ions, and interfacial components. (b) Concentration dependence of ionic conductivity and viscosity at 25 and 0 °C for NaPF_6 in EC/PC electrolyte. (c) Cyclic capability of NIBs using electrolytes with different concentrations at a current rate of 0.3C (30 mA g⁻¹) at 25 °C.

Received: February 14, 2020

Accepted: March 11, 2020

Published: March 11, 2020



as an example to investigate the change rule of physicochemical properties. In Figure 1b, the ionic conductivity accords with a downward-parabola-like relationship to the concentration, i.e., the higher the concentration, the slower the rate of increase in conductivity, affected by the ionic carrier number and mobility. The change of the ion conductivity with the growth of the concentration at the lower temperature is smaller than that at the higher temperature. Viscosity grows in an upward-parabola-like way with the concentration increase, which undergoes more dramatic change at lower temperature. Figure 1c further compares the electrochemical performances of the standard Na-ion full cells based on the disordered carbon anode and layered O3-Na[$\text{Cu}_{1/9}\text{Ni}_{2/9}\text{Fe}_{1/3}\text{Mn}_{1/3}$]O₂ cathode,⁹ using the aforementioned electrolytes with different concentrations. The 0.3 M electrolyte (abbr. ULCE) provides the highest specific capacity (~ 119 mAh/g) among the 0.1–0.5 M electrolytes at a moderate rate (0.3C, the most common rate in practical applications). Further reducing the concentration results in the capacity retention decay, as seen for 0.1 or 0.2 M electrolyte. Although the NIB using the 1 M electrolyte (abbr. CCE) exhibits a higher specific capacity (~ 121 mAh/g), the average Columbic efficiency is lower (~ 98 – 99%) than that using the low-concentration electrolytes ($\sim 99.9\%$) during cycling, indicating an unstable cycling process. Therefore, the ULCE is selected for the following detailed analysis.

In order to detect the kinetics limit of the ULCE, rate tests from 0.1C to 2C were carried out. In Figure S2, the ULCE can support 1C rate (~ 106 mAh/g@0.3 M vs ~ 117 mAh/g@1 M) but capacity decay occurs (more obvious at 2C). However, this problem can be solved via asymmetric cycling protocols, i.e., slow charge and fast discharge. In Figure S3, ULCE can provide a better capacity retention in 0.1C charge–0.5C discharge and show a similar capacity to that of CCE in 0.3C charge–1C discharge. Moreover, the performance was evaluated at lower temperature with slow kinetics. In Figure 2a, the initial Columbic efficiency (ICE) of the NIB slightly

improves from 25 to 0 °C, indicating a favorable battery formation process at the low temperature. More surprisingly, the capacity gap of the NIBs between using the ULCE and CCE shrinks and the ULCE even delivers a slightly better capacity retention (96%@0.3 M vs 95%@1 M) after 50 cycles at 0.3C at 0 °C in Figure 2b. The low viscosity of the ULCE at 0 °C presents a good wettability for the high-mass loading electrodes, compensating its low ionic conductivity (Figure 1b). An asymmetric cycling protocol can also improve the power density at 0 °C (Figure S4). We further reduced the operating temperature to -30 °C and surprisingly found that the NIB using the ULCE can even deliver more reversible capacity (~ 110 mAh/g) than that using the CCE (~ 55 mAh/g) at 0.05C (Figure S5), suggesting the fast kinetics of this ULCE at the extreme temperature. In contrast, when operating the NIB at the high temperature, thermodynamic stability rather than the kinetics issue is the key factor to be considered. In Figure 2a, the NIB using the ULCE exhibits a higher ICE ($\sim 80\%$) than that using the CCE ($\sim 72\%$) at 55 °C because of the less active Na⁺ loss and electrolyte decomposition to form the solid electrolyte interphase (SEI).^{10,11} Furthermore, the cycling instability of the CCE-based NIB is aggravated at high temperature (poor average Columbic efficiency), and the capacity retention is just 86% (vs $\sim 95\%$ @0.3 M) after 50 cycles at 0.3C in Figure 2b. Instead, the ULCE can support a very stable long cycling ($\sim 97\%$ @0.3 M vs $\sim 78\%$ @1 M, after 130 cycles) at the high rate of 1C because of the enhanced kinetics at 55 °C (Figure S6).

The X-ray photoelectron spectroscopy (XPS) measurements were performed to investigate the SEI on anodes and cathode electrolyte interphase (CEI) on cathodes. As summarized in Figure 2c, d and Tables S1 and S2, the atomic ratios of C plus O elements using the ULCE are higher than that using the CCE while the atomic ratios of P plus F elements using the ULCE are lower than that using the CCE, both of which conform to SEI and CEI films formed at different temperatures. This indicates that the SEI and CEI films in ULCE are prone to contain more organic components but less inorganic species than those at CCE. The organic and inorganic components are mainly derived from the decomposition of the solvents (EC/PC) and the anion from NaPF₆ salt, respectively, according to the electrical double-layer theory (Figure S7).¹² The hydrolysis products (HF, etc.) from PF₆[−] usually destroy the electrode structure and reduce the electrode stability (more serious at high temperatures).^{13,14} Thus, decreasing the amount of active NaPF₆ will enhance the thermodynamic stability of NIBs at high temperature. In addition, the ULCE induces organic-dominated SEI/CEI, because of the high molar ratio of solvent to salt (Figures S8 and 1a), and may provide favorable kinetics attributed to the formed porous oligomers and elastic alkyl carbonates, considering NaF may not be a fast ionic conductor,¹⁵ which explains the better low-temperature performance. Furthermore, the composition changes with the etching time (depth) and temperatures are both smaller for SEI/CEI formed in the ULCE than that in the CCE (Figure S9), demonstrating the uniform formation of interphases which are stable against the extreme temperatures.

In conclusion, we surprisingly find that NIBs can work well in such ultralow-concentration electrolyte (0.3 M) and demonstrate unexpected advantages. The dilute concentration not only reduces the cost significantly but also expands the working temperature range (-30 to 55 °C) for durable NIBs.

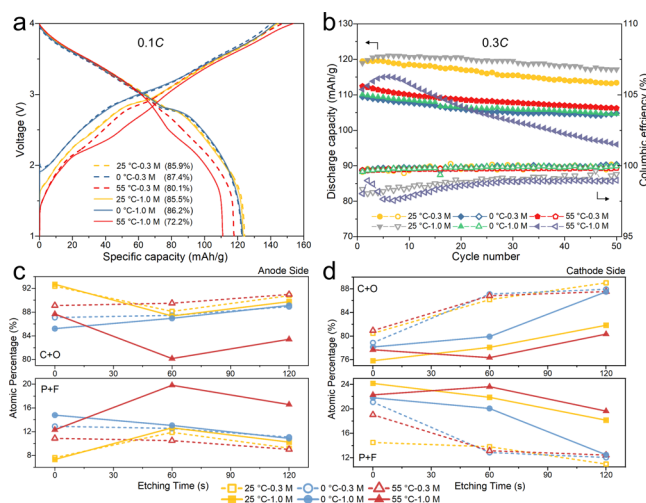


Figure 2. (a and b) Electrochemical performance of NIBs using ULCE or CCE at 0 °C, 25 and 55 °C. (a) Galvanostatic initial discharge/charge curves at 0.1C. The related ICEs are noted in parentheses. (b) Cyclic capability at 0.3C. (c and d) Surface passivation chemistry after one cycle of NIBs at 0.1C from XPS experiments with Ar⁺ etching. Atomic ratios of C (C 1s) plus O (O 1s) and P (P 2p) plus F (F 1s) elements detected at (c) the SEI films and (d) the CEI films.

Low viscosity and less corrosive risk (less HF attack) would help improve the interfacial wettability and Columbic efficiency at low and high temperatures, respectively. Moreover, the formed stable organic-dominated SEI/CEI with superior kinetics enables the stable operation of NIBs at extreme temperatures. The new dilute electrolyte chemistry is expected to extend to other electrolyte systems used in low-cost rechargeable batteries. Effective additives can further improve the performance of the ultralow-concentration electrolyte from bulk and interface regulation in the future.

■ ASSOCIATED CONTENT

Supporting Information

The Supporting Information is available free of charge at <https://pubs.acs.org/doi/10.1021/acsenerylett.0c00337>.

Experimental details, supplementary notes, asymmetric cycling protocols, cycling curves at -10 and -30 °C, rate capability at 55 °C, and detailed XPS data (PDF) (PDF)

■ AUTHOR INFORMATION

Corresponding Authors

Yaxiang Lu – Key Laboratory for Renewable Energy, Beijing Key Laboratory for New Energy Materials and Devices, Beijing National Laboratory for Condensed Matter Physics, Institute of Physics, Chinese Academy of Sciences, Beijing 100190, China; Yangtze River Delta Physics Research Center Co. Ltd., Liyang 213300, China; orcid.org/0000-0001-5202-175X; Email: yxlu@iphy.ac.cn

Yong-Sheng Hu – Key Laboratory for Renewable Energy, Beijing Key Laboratory for New Energy Materials and Devices, Beijing National Laboratory for Condensed Matter Physics, Institute of Physics, Chinese Academy of Sciences, Beijing 100190, China; College of Materials Science and Optoelectronic Technology, University of Chinese Academy of Sciences, Beijing 100049, China; Yangtze River Delta Physics Research Center Co. Ltd., Liyang 213300, China; orcid.org/0000-0002-8430-6474; Email: yshu@iphy.ac.cn

Authors

Yuqi Li – Key Laboratory for Renewable Energy, Beijing Key Laboratory for New Energy Materials and Devices, Beijing National Laboratory for Condensed Matter Physics, Institute of Physics, Chinese Academy of Sciences, Beijing 100190, China; College of Materials Science and Optoelectronic Technology, University of Chinese Academy of Sciences, Beijing 100049, China; orcid.org/0000-0003-1501-1549

Yang Yang – Key Laboratory for Renewable Energy, Beijing Key Laboratory for New Energy Materials and Devices, Beijing National Laboratory for Condensed Matter Physics, Institute of Physics, Chinese Academy of Sciences, Beijing 100190, China; College of Materials Science and Optoelectronic Technology, University of Chinese Academy of Sciences, Beijing 100049, China

Quan Zhou – Key Laboratory for Renewable Energy, Beijing Key Laboratory for New Energy Materials and Devices, Beijing National Laboratory for Condensed Matter Physics, Institute of Physics, Chinese Academy of Sciences, Beijing 100190, China; College of Materials Science and Optoelectronic Technology, University of Chinese Academy of Sciences, Beijing 100049, China; Yangtze River Delta Physics Research Center Co. Ltd., Liyang 213300, China

Xingguo Qi – Key Laboratory for Renewable Energy, Beijing Key Laboratory for New Energy Materials and Devices, Beijing National Laboratory for Condensed Matter Physics, Institute of Physics, Chinese Academy of Sciences, Beijing 100190, China; College of Materials Science and Optoelectronic Technology, University of Chinese Academy of Sciences, Beijing 100049, China; Yangtze River Delta Physics Research Center Co. Ltd., Liyang 213300, China

Qingshi Meng – Key Laboratory for Renewable Energy, Beijing Key Laboratory for New Energy Materials and Devices, Beijing National Laboratory for Condensed Matter Physics, Institute of Physics, Chinese Academy of Sciences, Beijing 100190, China; College of Materials Science and Optoelectronic Technology, University of Chinese Academy of Sciences, Beijing 100049, China; Yangtze River Delta Physics Research Center Co. Ltd., Liyang 213300, China

Xiaohui Rong – Key Laboratory for Renewable Energy, Beijing Key Laboratory for New Energy Materials and Devices, Beijing National Laboratory for Condensed Matter Physics, Institute of Physics, Chinese Academy of Sciences, Beijing 100190, China

Liquan Chen – Key Laboratory for Renewable Energy, Beijing Key Laboratory for New Energy Materials and Devices, Beijing National Laboratory for Condensed Matter Physics, Institute of Physics, Chinese Academy of Sciences, Beijing 100190, China; College of Materials Science and Optoelectronic Technology, University of Chinese Academy of Sciences, Beijing 100049, China; Yangtze River Delta Physics Research Center Co. Ltd., Liyang 213300, China

Complete contact information is available at:

<https://pubs.acs.org/doi/10.1021/acsenerylett.0c00337>

Author Contributions

[†]Y.L. and Y.Y. contributed equally.

Notes

The authors declare no competing financial interest.

■ ACKNOWLEDGMENTS

This work was supported by the National Natural Science Foundation of China (51725206) and the Strategic Priority Research Program of the Chinese Academy of Sciences (XDA21070500).

■ REFERENCES

- (1) Suo, L.; et al. *Nat. Commun.* **2013**, *4*, 1481.
- (2) Suo, L.; et al. *Science* **2015**, *350* (6263), 938.
- (3) Cao, X.; et al. *ACS Energy Letters* **2019**, *4* (10), 2529–2534.
- (4) Borodin, O.; et al. *Joule* **2020**, *4* (1), 69–100.
- (5) Kim, D.-H.; et al. *ACS Energy Letters* **2019**, *4* (6), 1265–1270.
- (6) Hu, Y.-S.; et al. *ACS Energy Letters* **2019**, *4* (11), 2689–2690.
- (7) Li, Y.; et al. *Chem. Soc. Rev.* **2019**, *48* (17), 4655–4687.
- (8) Li, Y.; et al. *Advanced Science* **2015**, *2* (6), 1500031.
- (9) Mu, L.; et al. *Energy Storage Science and Technology* **2016**, *5* (3), 324.
- (10) Ponrouch, A.; et al. *J. Mater. Chem. A* **2015**, *3* (1), 22–42.
- (11) Li, Y.; et al. *Adv. Energy Mater.* **2019**, *9* (48), 1902852.
- (12) Zhou, Y.; et al. *Nat. Nanotechnol.* **2020**, *15* (3), 224–230, DOI: [10.1038/s41565-019-0618-4](https://doi.org/10.1038/s41565-019-0618-4).
- (13) Han, J.-G.; et al. *Adv. Mater.* **2019**, *31* (20), 1804822.
- (14) Li, Y.; et al. *Chin. Phys. B* **2020**, *29* (4), 048201 DOI: [10.1088/1674-1056/ab7906](https://doi.org/10.1088/1674-1056/ab7906).
- (15) Yildirim, H.; et al. *ACS Appl. Mater. Interfaces* **2015**, *7* (34), 18985–18996.